ELSEVIER

International Journal of Mass Spectrometry 214 (2002) 95–104

International Journal of Mass Spectrometry

www.elsevier.com/locate/ijms

Application of mobility theory to the interpretation of data generated by linear and RF excited ion mobility spectrometers

Glenn E. Spangler[a,*], Raanan A. Miller[b,1]

[a] *Technispan LLC, 1133C Greenwood Road, Pikesville, MD 21208, USA*
[b] *Charles Stark Draper Laboratory, Cambridge, MA 02139, USA*

Received 16 July 2001; accepted 19 November 2001

Abstract

The theory of operation for linear and radio-frequency (RF)-ion mobility spectrometer (IMS) is briefly summarized. The operation of the linear IMS is best described by the continuity equation, and the operation of the RF-IMS is best described by the momentum balance equation. Simple relationships for the RF-IMS show that the compensation field is directly proportional to ion mobility, along with the cube of the dispersion field. When the relationships are applied to the analysis of field-asymmetric ion mobility spectrometry (FAIMS) data collected on a chloride ion, the ion is found to be non-converting (i.e., not clustered with water or nitrogen adducts). For this reason, the chloride ion might be used under controlled conditions to anchor the mobility scale for RF-IMS. Contributions of the electric field to the effective ion temperature influence not only the mobility of the ion, but also its cluster activity. (Int J Mass Spectrom 214 (2002) 95–104) © 2002 Published by Elsevier Science B.V.

Keywords: Ion mobility spectrometry (IMS); RF-IMS; FAIMS; Mobility theory

1. Introduction

Ion mobility spectrometry (IMS) was introduced as a ion separator in the early 1970s to provide a new dimension for gas chromatographic and mass spectrometric analyses [1]. In reality, the technique was not new [2], but rather its application. Combining the soft ionization capabilities of a radioactive ionization source with the ion separation capabilities of a linear drift tube was revolutionary in concept, and powerful in application [3,4]. The radioactive ionization source ionized the sample with high efficiency, and the drift tube facilitated miniaturization of the device for rugged field use. The ion mobilities were measured in the limit of low E/N, the ratio of the electric field strength (E) to the gas number density (N) for the drift gas.

As E/N increases, ion mobilities deviate measurably from their low field limit. For a uniform gas density, early dimensional analyses of the Boltzmann equation showed that ion mobility varies inversely as the square root of the electric field assuming a constant mean free path, or independently of the electric field assuming a constant mean free time [5]. Since then, the Boltzmann equation has been more extensively studied using perturbation (low field) and moment methods (high field),

* Corresponding author. E-mail: gspan@aol.com
[1] Present address: Sionex Corporation, 70 Walnut St., Wellesley Hills, MA 02481, USA.

1387-3806/02/$20.00
PII S1387-3806(01)00566-8

and ion mobility $K(\bar{\varepsilon})$ has been found to satisfy [6,7]

$$K(\bar{\varepsilon}) = \frac{3q}{8N}\left(\frac{\pi}{2\mu k_B T_{\text{eff}}}\right)^{1/2} \frac{1+\alpha}{\bar{\Omega}^{(1,1)}(\bar{\varepsilon})} \tag{1.1}$$

where q is the ionic charge, N the neutral gas density, μ the reduced mass for the ion, k_B is Boltzmann's gas constant, α is a correction term, $\bar{\Omega}^{(1,1)}(\bar{\varepsilon})$ is the collision cross-section averaged over a distribution of relative energies, and [8]

$$\bar{\varepsilon} = \tfrac{3}{2}k_B T_{\text{eff}} = \tfrac{3}{2}k_B T + \tfrac{1}{2}Mv_d^2(1+\beta) \tag{1.2}$$

is the mean relative energy, where T is the temperature of the drift gas, M the mass for the colliding neutral gas molecule, v_d the drift velocity for the ion, and β is another correction term. The dependence of $K(\bar{\varepsilon})$ on T_{eff} causes the reduced mobility $K_0(E)$ to satisfy [9]

$$K_0(E) = K_0^{(0)}\left[1 + \alpha_2\left(\frac{E}{N}\right)^2 + \alpha_4\left(\frac{E}{N}\right)^4 + \cdots\right] \tag{1.3}$$

where $K_0^{(0)}$ is adjusted to a gas *number density* ($N_0 = 2.686763 \times 10^{25}\,\text{m}^3$, known as the Loschmidt constant) corresponding to standard temperature and pressure, and α_2, α_4, etc. are constants independent of E/N. The correction terms in Eqs. (1.1) and (1.2) add approximately 10% to the accuracy of the equations.

Arguing from Eq. (1.3), Buryakov et al. introduced a new way to separate ions based on ion mobility [10]. The ions were submitted to an asymmetric radio-frequency (RF) field as they were transported through two parallel plates by a flowing drift gas [11,12]. Due to the imposed RF field, the ions were deflected perpendicular to the general motion created by the flowing drift gas, with the deflection being greater in one direction than in the other. As a result of the imbalanced deflections, the ions hit one or the other of the plates before they passed through the device. To prevent the loss, Buryakov et al. superimposed a dc compensation potential upon the asymmetric potential to redirect the motion of ions. For a given asymmetric RF excitation, they found that the magnitude for the dc compensation potential depended upon the ion. They were able to generate an ion mobility spectrum by scanning the dc compensation potential.

Viehland et al. have collected data on the ability of the (high) field-asymmetric ion mobility spectrometry (FAIMS) variant of RF-IMS to transmit chloride ions [13]. This was accomplished by varying the RF dispersion potential and recording the compensation potential needed to allow maximum transmission of ions through the device. The data were fitted to

$$\sum_{k=0}^{\infty} c_k \int_0^{2\pi} E^{2k+1}(\theta)\,\mathrm{d}\theta = 0 \tag{1.4}$$

a relationship thought necessary if the ions were to pass through the device. In Eq. (1.4), E is the electric field (sum of the fields created by the RF and dc potentials) applied across the parallel plates, $\theta = \omega t$ is the periodicity of the RF field and the c_k's are constants. With moderate success, Eq. (1.4) seemed to describe the data. Since the calculated mobility values agreed with previously published data [14], Viehland et al. felt FAIMS (in combination with mass spectrometry) was a good way to measure the high field mobility of identified ions in gases.

In this paper, another approach to analyzing Viehland et al.'s FAIMS chloride ion data is presented that allows additional information to be obtained from their experimental results.

2. Theoretical development

Fig. 1 shows, a simplified schematic for the drift tube of an IMS. The schematic could represent either a cylindrical linear drift tube using a longitudinal dc field to separate ions [3,4], or two plates of a RF-IMS using a transverse asymmetric field to separate ions [10]. The ion source introduces ions into one end of the tube, and an ion collector receives the ions at the other end of the tube. The flow of ions from source to collector is controlled by either an electric field (linear IMS) or a flow of drift gas (RF-IMS). The $\hat{z}$-axis is chosen to lie along the symmetry axis of the drift tube ($z = 0$ corresponding to the location of the source), and the $\hat{x}$-axis is perpendicular to that symmetry axis.

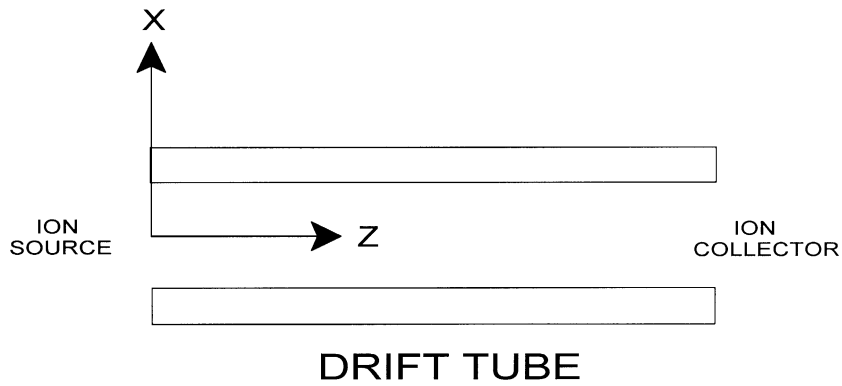

Fig. 1. Simplified schematic for an ion mobility spectrometer drift tube.

Two approaches can be taken to theoretically describe ion motion occurring within the drift tube. The first is to write down and find a solution to the continuity equation [15–20]

$$\frac{\partial n_{\mathrm{T}}}{\partial t} - \sum_i \vec{\nabla} \cdot x_i \overleftrightarrow{D}_i \cdot \vec{\nabla} n_{\mathrm{T}} + \sum_i x_i \vec{v}_{\mathrm{d}i} \cdot \vec{\nabla} n_{\mathrm{T}} + \sum_i x_i \alpha_i n_{\mathrm{T}} = 0 \tag{2.1}$$

where n_{T} is the total ion concentration within an exchanging ion mixture migrating in local equilibrium through the drift tube, x_i is the relative concentration of the ith ion in the mixture, $\overleftrightarrow{D}_i$ is the diffusion tensor, $\vec{v}_{\mathrm{d}i}$ is the drift velocity and α_i is the rate of ion loss by means other than cluster exchange reactions (e.g., by loss of charge). Eq. (2.1) provides an exact description of ion behavior as long as ion density gradients are small and higher order terms (skewness, kurtosis, etc.) can be neglected. Estimates of ion density gradients can be made in advance, so that the validity of the equation is not obtained a posteriori.

A statistical mechanical version of Eq. (2.1) shows that, in principle, all the variables are time-dependent [21]. This leads to a considerably complex solution for the ion concentration, even when a delta function is used to simulate the introduction of ions into the device [22]. Since most linear IMSs are operated under "quasi-homogeneous" conditions where x_i, $\overleftrightarrow{D}_i$, $\vec{E}$, $\vec{v}_{\mathrm{d}i}$ and α_i are independent of the spatial coordinates, the spatial distribution of the ion concentration can be described by a difference in error functions that generates a Gaussian when the pulse width applied to the shutter grid is narrowed [17]. The centroid for the Gaussian travels through the drift tube in accordance with

$$l = \sum_i x_i \vec{v}_{\mathrm{d}i} t \tag{2.2}$$

where l is the location of the centroid along the $\hat{z}$-axis at time t. Unlike linear IMS, Eq. (2.1) is not as well suited for describing ion motion in an RF-IMS because x_i, $\overleftrightarrow{D}_i$, $\vec{E}$, $\vec{v}_{\mathrm{d}i}$ and α_i are functions of drift time.

The second approach to describing ion motion within an IMS is to equate the forces applied to the ion and find a solution to the resulting equation of motion [20,23]. Assuming the ion is a non-converting ion with a mass m, the equation of motion is

$$m\frac{\mathrm{d}^2 \vec{r}}{\mathrm{d}t^2} + \mu\nu(\bar{\varepsilon})\frac{\mathrm{d}\vec{r}}{\mathrm{d}t} - q\vec{E} = 0 \tag{2.3}$$

where $\nu(\bar{\varepsilon})$ is the collision frequency for the ion (dependent on ion energy $\bar{\varepsilon}$) and $\vec{r}$ is the location of the ion as it responds to the applied electric field $\vec{E}$. In writing down Eq. (2.3), spatial uniformity is assumed so that the random energy induced in the direction of motion ($k_{\mathrm{B}}T_{||}$) can be neglected [22]. Except for

this assumption, Eq. (2.3) is entirely consistent with momentum-transfer theory [20,23–25]. It is particularly suited for describing ion motion in a RF-IMS because the electric field appears explicitly within the relationship. Since the motion imposed upon the ion by the flowing drift gas is not included, Eq. (2.3) must be modified.

Using manipulations frequently applied by momentum-transfer theory (although ancillary to it), Eq. (2.3) can be rearranged and $\mathrm{d}\vec{r}/\mathrm{d}t$ equated to the drift velocity $\vec{v}_\mathrm{d}$

$$\vec{v}_\mathrm{d} = \frac{q}{\mu\nu(\bar{\varepsilon})}\vec{E} - \frac{m}{\mu\nu(\bar{\varepsilon})}\frac{\mathrm{d}\vec{v}_\mathrm{d}}{\mathrm{d}t} \tag{2.4}$$

This velocity is relative to a coordinate system moving with the linear velocity of the drift gas. The motion can be referenced to the laboratory frame of reference (shown fixed to the ion source in Fig. 1) by adding the drift gas velocity $\vec{v}_\mathrm{g}$ to $\vec{v}_\mathrm{d}$, so that Eq. (2.4) can be written as

$$\vec{v}_\mathrm{dg} = \vec{v}_\mathrm{g} + \frac{q}{\mu\nu(\bar{\varepsilon})}\vec{E} - \frac{m}{\mu\nu(\bar{\varepsilon})}\frac{\mathrm{d}\vec{v}_\mathrm{d}}{\mathrm{d}t} \tag{2.5}$$

where $\vec{v}_\mathrm{dg} = \vec{v}_\mathrm{g} + \vec{v}_\mathrm{d}$.

A RF-IMS is generally operated under the conditions

$$\vec{v}_\mathrm{g} = v_\mathrm{g}\hat{z} = \frac{\dot{Q}_\mathrm{d}}{A_\mathrm{c}}\hat{z}, \qquad \vec{E} = E_\mathrm{D}(\omega, t)\hat{x} \tag{2.6}$$

where $\dot{Q}_\mathrm{d}$ is the volumetric flow of drift gas (sometimes referred to as a carrier gas), A_c the cross-sectional area of the flow channel within the drift tube, and $E_\mathrm{D}(\omega, t)$ is the electric field that varies with frequency ω and time t. When the relationships of Eq. (2.6) are combined with Eq. (2.5), the component equations become

$$\begin{aligned}
&\hat{z}\text{-component} \quad v_{\mathrm{dg},z} = v_\mathrm{g},\\
&\hat{x}\text{-component} \quad v_{\mathrm{dg},x} = \frac{q}{\mu\nu(\bar{\varepsilon})}E_\mathrm{D}(\omega, t)\\
&\qquad\qquad\qquad - \frac{m}{\mu\nu(\bar{\varepsilon})}\frac{\mathrm{d}v_{\mathrm{dg},x}}{\mathrm{d}t}
\end{aligned} \tag{2.7}$$

Eq. (2.7) states that the ions are transported along the $\hat{z}$-axis by the flowing drift gas and oscillate in the $\hat{x}$-direction due to excitation by the applied RF field. While the $\hat{z}$-direction motion is important, particularly as is relates to Poiseuille flow and the possibility for the development of turbulence, the remainder of this paper will address the $\hat{x}$-motion.

Two approaches can be taken to exciting the $\hat{x}$-motion. These are to apply an asymmetric *rectangular* waveform to the dispersion electrodes where the time integral of the waveform is set equal to zero [10], or to apply an asymmetric *sinusoidal* waveform along with its second harmonic to the dispersion electrodes where the amplitude for the second harmonic is half the amplitude for the primary (FAIMS) [11,26]. For a high excitation potential, the asymmetric waveforms cause the ions to migrate towards one or the other of the dispersion electrodes, hit the dispersion electrode, and be lost as a contributor to the ion current passing through the device. Applying a bucking dc potential arrests the migratory motion so the ions can once again pass through the device.

In Eq. (2.7), the "$\hat{x}$-component" motion is not only regulated by a term depending on the RF field, but also by a term functionally dependent upon the first derivative of the ion velocity. Both terms are preceded by a coefficient that is inversely proportional to the collision frequency $\nu(\bar{\varepsilon})$

$$\nu(\bar{\varepsilon}) = N\bar{v}_\mathrm{r}Q_\mathrm{D}(\bar{\varepsilon}) \tag{2.8}$$

where $\bar{v}_\mathrm{r}$ is the relative velocity associated with the collision dynamics and $Q_\mathrm{D}(\bar{\varepsilon})$ is the momentum-transfer or diffusion cross-section. Since the collision frequency is directly proportional to gas density, it decreases with the pressure of the carrier gas flowing through the RF-IMS. This allows Eqs. (2.3) and (2.7) to assume the form of the Mathieu equation (assuming appropriate RF-excitation) at sufficiently reduced pressure. For this reason, the performance of a RF-IMS has been compared to a collisionally damped quadruple mass filter [27–29]. The effects of collisions become important in approximately the 0.1–1.3 Pa (10^{-3} to 10^{-2} Torr) range.

Because of this analogy of the RF-IMS with the quadruple mass filter, it is important to show that the second term of Eq. (2.7) is negligible when the

RF-IMS is operated under atmospheric pressure conditions. For a RF-IMS excited with an asymmetric *rectangular* potential, this follows immediately because the trajectory followed by the ion is zig-zagged and the first derivative of the velocity associated with the motion is equal to zero. For a RF-IMS excited with an asymmetric *sinusoidal* potential, the first derivative of the velocity is not zero, but *sinusoidal*. The average of the *sinusoidal* derivative, however, is zero, allowing it to make a negligible contribution to the overall operation of the RF-IMS. Furthermore if the drift velocity of the ion is assumed to oscillate with a frequency ω, the coefficient $m\omega/\mu\nu(\bar{\varepsilon})$ is much less than one for the 210 kHz to 1.0 mHz frequencies typically used to excite a RF-IMS [30]. Thus, the second term is negligible regardless of the method of excitation, *rectangular* or *sinusoidal*, and the $\hat{x}$-motion for the ion is reasonably described by

$$v_{\mathrm{dg},x} = \frac{q}{\mu\nu(\bar{\varepsilon})} E_{\mathrm{D}}(\omega, t) = K(\bar{\varepsilon}) E_{\mathrm{D}}(\omega, t) \tag{2.9}$$

where $K(\bar{\varepsilon})$ is the mobility of the ion. If instead of being non-converting, the ion converts to another ion that is traveling in *local equilibrium* with it, Eq. (2.9) becomes [31]

$$v_{\mathrm{dg},x} = \sum_i x_i K_i(\bar{\varepsilon}_i) E_{\mathrm{D}}(\omega, t) \tag{2.10}$$

where x_i is the partial fraction of the ith species already described in connection with Eqs. (2.1) and (2.2).

The transition from Eqs. (2.7) to (2.9) has historical significance. Eq. (2.7) is a phenomenological relationship that is consistent with momentum-transfer theory, but not studied much until recently [22]. Eq. (2.9) is the basic statement of momentum-transfer theory and has been studied for more than 50 years. For this reason, when the first derivative was eliminated in Eq. (2.7), the discussion moved from a phenomenological to a more mainstream description of ion mobility. From ion mobility theory, it is known that the left-side of Eq. (2.9) describes the momentum lost by the ions as they undergo ion-neutral collisions, the right-side describes momentum gained by the ions from the electric field, and the first derivative of Eq. (2.7) describes the gain or loss in momentum due to the difference. The ion mobility, $K_i(\bar{\varepsilon}_i)$, in Eq. (2.10) is the same as in Eq. (1.1) with the intensive variables containing ion specific information.

Since it can be argued that the ions in an RF-IMS are at different temperatures at different points in their trajectory, the thermal properties of Eq. (2.10) must be studied. This is accomplished by differentiating Eq. (2.10) with respect to temperature to yield

$$\frac{\mathrm{d}v_{\mathrm{dg},x}}{\mathrm{d}T} = \sum_i \frac{\mathrm{d}[x_i K_i(\bar{\varepsilon}_i)]}{\mathrm{d}T} E_{\mathrm{D}}(\omega, t) \tag{2.11}$$

Since momentum-transfer theory states that ion mobility (and hence drift velocity) scales not only with gas temperature, but also with electric field [32]; Eq. (2.11) can rewritten as

$$\frac{\mathrm{d}v_{\mathrm{dg},x}}{\mathrm{d}T_{\mathrm{eff}}} = \sum_i \frac{\mathrm{d}[x_i K_i(\bar{\varepsilon}_i)]}{\mathrm{d}T_{\mathrm{eff}}} E_{\mathrm{D}}(\omega, t) \tag{2.12}$$

where T_{eff} is the effective temperature of the ion

$$T_{\mathrm{eff}} = T + \frac{M v_{\mathrm{dg},x}^2}{3k_{\mathrm{B}}}(1 + \beta') \tag{2.13}$$

Because Eq. (2.12) describes the motion of an exchanging ion mixture migrating in local equilibrium, β in Eq. (1.2) has been replaced by β' in Eq. (2.13) to acknowledge that β is a function of the drift velocity, and the drift velocity of an exchanging ion mixture is different from a single ion [33]. After introducing Eq. (2.10) into Eq. (2.13) and substituting Eq. (2.13) into Eq. (2.12), Eq. (2.12) becomes

$$\mathrm{d}v_{\mathrm{dg},x} = \frac{2M}{9k_{\mathrm{B}}} \left(\frac{\mathrm{d}\log\left(\sum_i x_i K_i(\bar{\varepsilon}_i)\right)}{\mathrm{d}T_{\mathrm{eff}}} \right) \times \mathrm{d}\left[\left(\sum_i x_i K_i(\bar{\varepsilon}_i) \sqrt{1+\beta'} E_{\mathrm{D}} \right)^3 \right] \tag{2.14}$$

after rearrangement. Eq. (2.14) is a relationship between two differentials, $\mathrm{d}v_{\mathrm{dg},x}$ and $\mathrm{d}[(\sum_i x_i K_i(\bar{\varepsilon}_i) \sqrt{1+\beta'} E_{\mathrm{D}})^3]$, with a proportionality constant functionally dependent on T_{eff}. Values for $\mathrm{d}\log K_0/\mathrm{d}T_{\mathrm{eff}}$ are compiled in tables of mobility data [33].

Another relationship for $dv_{dg,x}$ is the relationship it has with the complementary field E_C

$$dv_{dg,x} = -d\left[\sum_i x_i K_i(\bar{\varepsilon}_i) E_C\right] \tag{2.15}$$

When Eq. (2.15) is differentiated with respect to time, it satisfies

$$dv_{dg,x} = E_C \frac{d\left[\sum_i x_i K_i(\bar{\varepsilon}_i)\right]}{dt} dt + \sum_i x_i K_i(\bar{\varepsilon}_i) \frac{dE_C}{dt} dt \tag{2.16}$$

Because the complementary potential is a dc potential, the second term on the right is zero, and when Eq. (2.16) is combined with Eq. (2.14), it becomes

$$E_C\, dt = -\frac{M}{3k_B} \frac{d\left[\left(\sum_i x_i K_i(\bar{\varepsilon}_i)\sqrt{1+\beta'}\right)^2\right]}{dT_{eff}} E_D^3\, dt \tag{2.17}$$

A relationship between the complementary field and the cube of the dispersion field has just been derived.

3. Application

The desire is to now apply the theory developed in the previous section to the chloride ion data of Viehland et al. [13]. In order for this to happen, some assumptions must be made. The first is to assume that the chloride ion studied by Viehland et al. was a non-converting ion with $x_0 = 1$ and $x_i = 0$ for $i > 0$. Since this assumption corresponds to a bare ion stripped of its water adducts, it makes β' equal to β. The second assumption is that the first derivative of $K(\bar{\varepsilon})^2(1+\beta)$ relative to T_{eff} is a constant. Referring to Eq. (1.1), this corresponds to an ion whose $K(\bar{\varepsilon})\sqrt{1+\beta}$ product is directly proportional to $\sqrt{T_{eff}}$; or referring to Eq. (1.2), to an ion whose translational energy is significantly greater than $(3/2)k_B T$.

Applying the above assumptions, Eq. (2.17) can be integrated over one cycle of the RF potential

$$\int_{cycle} E_C\, dt = -\frac{M}{3k_B} \frac{d[K^2(\bar{\varepsilon})(1+\beta)]}{dT_{eff}} \int_{cycle} E_D^3\, dt \tag{3.1}$$

to yield

$$E_C = -\frac{M}{3k_B} \frac{d[K^2(\bar{\varepsilon})(1+\beta)]}{dT_{eff}} \overline{\int_{cycle} E_D^3(\omega, t)\, dt} \tag{3.2}$$

where

$$\overline{\int_{cycle} E_D^3(\omega, t)\, dt} \equiv \frac{\int_{cycle} E_D^3(\omega, t)\, dt}{\tau_{cycle}} \tag{3.3}$$

and τ_{cycle} is the period of the RF potential. Eq. (3.2) is a linear relationship between the compensation E_C and the cube of the dispersion $\overline{\int_{cycle} E_D^3(\omega, t)\, dt}$ fields with the slope containing ion specific information [11,34].

The asymmetric waveform used by Viehland et al. was [13]

$$E_D(\omega t) = \frac{D}{3d}\left[2\sin(\omega t) + \sin\left(2\omega t - \frac{\pi}{2}\right)\right] \tag{3.4}$$

where D is the high potential applied to the cylindrical dispersion electrodes separated by a distance d. For this waveform, $\overline{\int E_D^3(\omega, t)\, dt} = 3(D/3d)^3$ and Eq. (3.2) can be written as

$$E_C = -\frac{M}{k_B}\left(\frac{D}{3d}\right)^3 \frac{d[K^2(\bar{\varepsilon})(1+\beta)]}{dT_{eff}} \tag{3.5}$$

Fig. 2 shows, a plot of Viehland et al.'s compensation vs. dispersion potential data using Eq. (3.5) to fit them. As expected, a linear relationship exists. The plot has a slope of $-1.29 \times 10^{-3}\,V^{-2/3}$ with a negligible intercept of $-0.32\,V^{1/3}$. When Eq. (3.5) is applied to back calculate the slope using Viehland et al.'s approximated 2 mm gap and previously published chloride ion data, the slope is found to lie between -7×10^{-4} and $-8 \times 10^{-4}\,V^{-2/3}$ [13,33].

Finally, the above theory can be extended for general application to the interpretation of RF-IMS data. This is done by differentiating Eq. (3.2) with respect

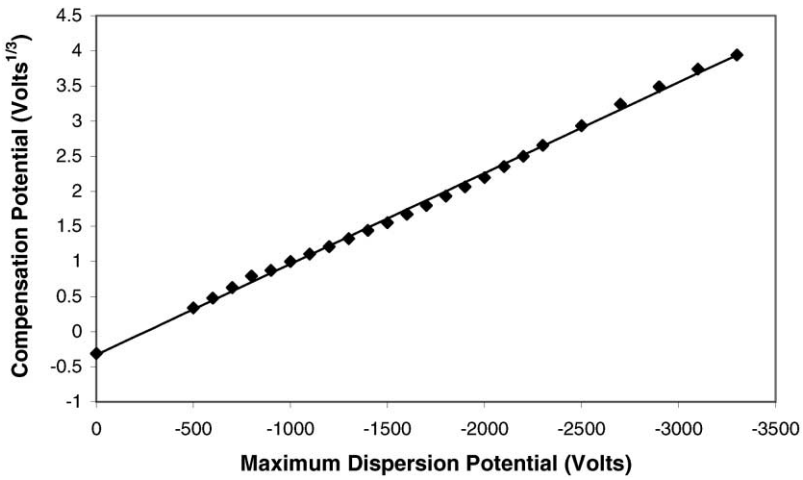

Fig. 2. A plot of the cube root of Viehland et al.'s compensation potential "$C(V)$" vs. the dispersion potential "$D(V)$" required to transmit chloride ions through their FAIMS RF-IMS. The straight line is given by $\sqrt[3]{C(V)} = -0.326 - 0.00129D(V)$ that fits the data with a 99.7% r^2-confidence.

to mobility (or more precisely $K(\bar{\varepsilon})\sqrt{1+\beta}$) and combining the result with Eq. (3.2). After a cancellation of terms, the result is

$$\frac{\mathrm{d}E_\mathrm{C}}{E_\mathrm{C}} = \frac{\mathrm{d}[K(\bar{\varepsilon})\sqrt{1+\beta}]}{K(\bar{\varepsilon})\sqrt{1+\beta}} \tag{3.6}$$

Eq. (3.6) states that the mobility of the ion is in direct proportion to the complementary field used to resolve the peaks. This is a very simple relationship that allows RF-IMS data to be compared with linear IMS data. Two things, however, can interfere. The first is Eq. (3.2) can revert back to Eq. (2.17) in the presence of solute (e.g., water) or a high concentration of sample molecules where x_i, $i > 0$, assumes non-zero values. The second is that the first derivative of $K(\bar{\varepsilon})^2(1+\beta)$ in Eqs. (2.17) and (3.2) becomes a function of temperature, not allowing it to be a constant due to variations, for example, in the collision cross-section. Possible examples of these latter phenomena exist, but they are not very well documented.

4. Thermochemistry

In Section 3, the chloride ions of Viehland et al.'s experiments were assumed to be non-converting ions. No justification for that assumption was given, except that it was needed to obtain the desired results. The purpose of this section is to more carefully confirm the assumption.

The reaction of significance is

$$\mathrm{Cl}^- + \mathrm{H_2O} \underset{k_\mathrm{r}}{\overset{k_\mathrm{f}}{\rightleftharpoons}} \mathrm{Cl}^-(\mathrm{H_2O}) \tag{4.1}$$

that has been studied by Kebarle and co-workers in the absence of an applied electric field [35,36]. If k_f and k_r are the forward and reverse rate constants, and K_equil is the equilibrium constant, then

$$K_\mathrm{equil} = \frac{k_\mathrm{f}}{k_\mathrm{r}} = \frac{[(\mathrm{H_2O})\mathrm{Cl}^-]}{[\mathrm{H_2O}][\mathrm{Cl}^-]} = \exp\left(-\frac{\Delta G^\circ_{0,1}}{RT}\right) \tag{4.2}$$

where the brackets indicate the concentration of the respective species in atmospheres, $\Delta G^\circ_{0,1}$ is the free energy change referenced to the standard state of one atmosphere, and R is the Rydberg gas constant. The measured enthalpy and entropy changes are -13.1 kcal/mol and -16.5 cal/mol-degree, respectively. To determine if cluster activity contributed to Viehland et al.'s experiments, it is necessary to investigate the kinetics, as well as the equilibrium, associated with Eqs. (4.1) and (4.2).

The forward rate constant k_f is reasonably approximated by the average dipole orientation (ADO) model for ion–molecule reactions [37]. The ADO model states

$$k_f = \pi \left[\left(\frac{4\alpha_p q^2}{\mu} \right)^{1/2} + \left(\frac{2q\mu_D}{\mu v_r} \right) \right] \tag{4.3}$$

where q is the ionic charge, α_p the polarizability, μ the reduced mass, μ_D the dipole moment for the water molecule, and v_r is the relative velocity at infinite separation between the reactants. For thermally averaged velocities, Eq. (4.3) can be restated as

$$\bar{k}_f = \left(\frac{2\pi q}{\mu^{1/2}} \right) \left[\alpha_p^{1/2} + c\mu_D \left(\frac{2}{\pi k_B T} \right)^{1/2} \right] \tag{4.4}$$

where $\bar{k}_f$ is a thermally averaged rate constant and c is an adjustable parameter to account for the average librational angle of the dipole. Since c is much less than one (0.05 ± 0.02), the term involving the dipole is generally small and $\bar{k}_f$ is independent of temperature. Typical values for k_f lie between 10^{-10} and 10^{-9} cm^3 per molecule s^{-1}.

Since the equilibrium constant is known, the reverse rate constant k_r is obtained by substituting k_f into Eq. (4.2) and solving for k_r. The result is

$$k_r = k_f \exp\left(\frac{\Delta G^\circ_{0,1}}{RT} \right) \tag{4.5}$$

Before Eqs. (4.2)–(4.5) can be applied to Viehland et al.'s data, an estimate must be made of the water concentration contained in their sample and carrier gases. They reported using compressed air processed through a "gas purification cylinder (charcoal/molecular sieve)", but did not otherwise report a water concentration. Additional contact with the group yielded the information that the compressed air was a gas cylinder of purified air and the charcoal/molecular sieve was activated at 250 °C with a purge of dry helium [38]. When these same procedures were followed to precondition the carrier and drift gases for a recent IMS/MS study on reactant ions, the measured water concentration in the carrier and drift gases was approximately 0.6 ppm [39].

Introducing 0.6 ppm for the water concentration into

$$\tau_f = \frac{0.693}{k_f\,[H_2O]}, \qquad \tau_r = \frac{0.693}{k_r\,[M]} \tag{4.6}$$

the forward and reverse time constants are found to be 470 and 240 ps, respectively, for a 300 K drift gas temperature and 10^{-10} cm^3 per molecule s^{-1} for k_f. Since field reversals occur in FAIMS every 1–20 μs, these times are short compared to the time required for field reversal, and allow equilibrium conditions to be continuously re-established throughout the flight of the ion. The possibility for the development of non-equilibrium conditions is not possible.

Introducing 0.6 ppm for the water concentration into Eq. (4.2), the concentration ratio of $(H_2O)Cl^-$ to Cl^- is found to be on the order of 0.5 again for a drift gas temperature of 300 K. This result suggests that Viehland et al.'s chloride ions were clustered with water molecules unless another mechanism can be identified to suggest otherwise. Fortunately for the arguments contained in this paper, this second mechanism is believed to be the stripping of the ion of its adducts when the ion is exposed to the high electric field used to excite the RF-IMS. Because ion–molecule reactions are involved, care must be taken when describing the nature of the equilibrium shift.Kumar et al. state that the stationary transport of a multicomponent system in chemical equilibrium can formally be treated as the transport of a one-species system provided adjustments are made to sum over all charged species to obtain the density and velocity distributions regardless of charge carrier [40]. This is accomplished by including a particle-conserving or non-reactive part, a reactive loss part, and a reactive gain part to the collision operator. When a sum is performed over all the charged species, the overall reaction rates are zero and Eq. (1.2) applies to the migrating charge.

Using this approach, we note that Viehland et al. worked with E/N values ranging from 10.21 to 66.15 Td [13]. If their ions were only the chloride ion, this would correspond to a maximum ion temperature of 450–2300 K, respectively [33]. But we

must entertain the idea that their ions also contained $(H_2O)Cl^-$. This is accomplished by using

$$v_d = \sum_i x_i v_{di} \tag{4.7}$$

for the drift velocity in Eq. (1.2), where the *i*-summation includes both the $(H_2O)Cl^-$ and Cl^- ions. To obtain the effective ion temperature, knowledge of the drift velocity for the $(H_2O)Cl^-$ ion is required. Although this type of information is not readily available, it might be argued that the contributions from the $(H_2O)Cl^-$ ion are negligible either because the collision cross-section for $(H_2O)Cl^-$ differs little from Cl^- ion, or $x_{(H_2O)Cl^-}$ is small due to the low water concentration used in Viehland et al.'s experiments. In either case, the effective ion temperature would only be slightly less than the 450–2300 K noted above.

When these adjusted ion temperatures are introduced into Eq. (4.2), the concentration ratios for $(H_2O)Cl^-$ to Cl^- are found to be 3.4×10^{-4} to 2.6×10^{-9}, respectively. Since these numbers are much less than one, the assumption that Viehland et al.'s chloride ions were not clustered with a water molecule appears to be valid. Of course, the conclusion strictly applies to the ions when they are at the extremes of their migratory motion. On the other hand, the ion temperatures are so high, and the concentration ratios so low, that the Cl^- ions cannot be clustered with water over a significant portion of their ion trajectory.

5. Conclusions

A summary of theoretical considerations has been presented that is applicable to the analysis of data generated by IMS. Larger portions of the considerations apply to a newer form of ion mobility spectrometry, namely RF-IMS. The compensation potential for a RF-IMS was shown to be proportional to the cube of the dispersion potential with the proportionality constant containing ion specific information. The theory states that if a plot of the cube root of the compensation potential is plotted against the dispersion potential, a straight line results for a non-converting ion.

Again for a non-converting ion, the relationship

$$\frac{dE_C}{E_C} = \frac{d[K(\bar{\varepsilon})\sqrt{1+\beta}]}{K(\bar{\varepsilon})\sqrt{1+\beta}} \tag{5.1}$$

applies to the interpretation of RF-IMS data. That is, the mobility of the ion is directly proportional to the complementary potential. Because Eq. (5.1) contains differentials, a calibrant ion is needed to anchor the mobility scale. An analysis of Viehland et al.'s chloride ion data suggests that the chloride ion is a non-converting ion under the conditions used to operate an RF-IMS, and is thus a good candidate to anchor the mobility scale. Proper care, however, must be taken to control experimental conditions (e.g., water concentration) to allow reproducibility.

Acknowledgement

Portions of this work were funded by The Charles Stark Draper Laboratory Inc., Cambridge, MA.

References

[1] M.J. Cohen, Plasma chromatography—a new dimension for gas chromatography and mass spectrometry, in: A. Zlatkis (Ed.), Advances in Chromatography, Chromatography Symposium, Houston, TX, 1970.
[2] P. Langevin, Ann. de Chimie et de Phys. 5 (1905) 205–288 (Translated in E.W. McDaniel, Collision Phenomena in Ionized Gases, Wiley, New York, 1964, Appendix II).
[3] T.W. Carr (Ed.), Plasma Chromatography, Plenum Press, New York, 1984.
[4] G.A. Eiceman, Z. Karpas, Ion Mobility Spectrometry, CRC Press, Boca Raton, FL, 1994.
[5] G.H. Wannier, Bell Syst. Tech. J. 32 (1953) 170–254.
[6] S. Chapman, T.G. Cowling, The Mathematical Theory of Non-Uniform Gases, Cambridge University Press, London, 1939, 1952, 1970.
[7] E.A. Mason, E.W. McDaniel, Transport Properties of Ions in Gases, Wiley, New York, 1988 (Chapter 5).
[8] E.A. Mason, E.W. McDaniel, Transport Properties of Ions in Gases, Wiley, New York, 1988, p. 149.
[9] E.A. Mason, E.W. McDaniel, Transport Properties of Ions in Gases, Wiley, New York, 1988, pp. 150–151.
[10] I.A. Buryakov, E.V. Krylov, E.G. Nazarov, U.K. Rasulev, Int. J. Mass Spectrom. Ion Proc. 128 (1993) 143–148.
[11] B.L. Carnahan, A.S. Tarassov US Patent 5,420,424 (1995).

[12] E.V. Krylov, Sov. Phys. Tech. Phys. 44 (1999) 113–116.
[13] L.A. Viehland, R. Guevremont, R.W. Purves, D.A. Barnett, Int. J. Mass Spectrom. 197 (2000) 123–130.
[14] H. Bohringer, D.W. Fahey, W. Lindinger, F. Howorka, F.C. Fehsenfeld, D.L. Albritton, Int. J. Mass Spectrom. Ion Proc. 81 (1987) 44–65.
[15] E.A. Mason, E.W. McDaniel, Transport Properties of Ions in Gases, Wiley, New York, 1988, pp. 86–91.
[16] J.T. Moseley, I.R. Gatland, D.W. Martin, E.W. McDaniel, Phys. Rev. 178 (1968) 234–239.
[17] G.E. Spangler, C.I. Collins, Anal. Chem. 47 (1975) 403–407.
[18] S.B. Woo, J.H. Whealton, Phys. Rev. 180 (1969) 314–319.
[19] K. Iinuma, Can. J. Chem. 69 (1991) 1090–1099.
[20] G.E. Spangler, Field Anal. Chem. Technol. 4 (2000) 255–267.
[21] T. Kihara, Rev. Mod. Phys. 24 (1952) 45–61.
[22] R.E. Robson, R.D. White, T. Makabe, Ann. Phys. 261 (1997) 74–113.
[23] S.L. Lin, L.A. Viehland, E.A. Mason, J.H. Whealton, J.N. Bardsley, J. Phys. B: Atom. Molec. Phys. 10 (1977) 3567–3575.
[24] E.A. Mason, E.W. McDaniel, Transport Properties of Ions in Gases, Wiley, New York, 1988, pp. 145–159.
[25] E.A. Mason, H.S. Hann, Phys. Rev. 5 (1972) 438–441.
[26] R. Guevremont, R.W. Purves, Rev. Sci. Instrum. 70 (1999) 1370–1383.
[27] P.H. Dawson (Ed.), Quadruple Mass Spectrometry and its Applications, Elsevier, Amsterdam, 1976.
[28] D.E. Goeringer, S.A. McLuckey, J. Chem. Phys. 104 (1996) 2214–2221.
[29] G.E. Spangler, US Patent 6,124,592.
[30] R.W. Purves, D.A. Barnette, R. Guevremont, Int. J. Mass Spectrom. 197 (2000) 163–177.
[31] J.M. Preston, L. Rajadhyax, J. Anal. Chem. 60 (1988) 31–34.
[32] E.A. Mason, E.W. McDaniel, Transport Properties of Ions in Gases, Wiley, New York, 1988, pp. 245–254, 289–290.
[33] L.A. Viehland, E.A. Mason, At. Data Nucl. Data Tables 60 (1995) 37–95.
[34] I.A. Buryakov, E.V. Krylov, A.L. Makas, E.G. Nazarov, V.V. Pervukhin, U.K. Rasulev, Sov. Tech. Phys. Lett. 17 (1991) 446–447.
[35] M. Arshadi, R. Yamdagni, P. Kebarle, J. Phys. Chem. 74 (1970) 1475–1482.
[36] P. Kebarle, Ann. Rev. Phys. Chem. 28 (1977) 445–476.
[37] M.T. Bowers, T. Su, Adv. Electron. Electron Phys. 34 (1973) 223–279.
[38] R. Guevremont, personal communication, 2001.
[39] G.E. Spangler, Int. J. Mass Spectrom. 208 (2001) 169–191.
[40] K. Kumar, H.R. Skullerud, R.E. Robson, Aust. J. Phys. 33 (1980) 343–448.